Available online at www.sciencedirect.com

ScienceDirect

Ceramics International 40 (2014) 1587–1591

CERAMICS INTERNATIONAL

www.elsevier.com/locate/ceramint

# Characterization and photocatalytic properties of nanoporous titanium dioxide layer fabricated on pure titanium substrates by the anodic oxidation process

T. Dikici[a,b,c,d], M. Erol[a,c,e,*], M. Toparli[a,b,f], E. Celik[a,b,f]

[a]Dokuz Eylul University, Department of Metallurgical and Materials Engineering, Buca 35160, Izmir, Turkey
[b]Dokuz Eylul University, Center for Fabrication and Application of Electronic Materials, EMUM, Buca 35160, Izmir, Turkey
[c]Dokuz Eylul University, The Graduate School of Natural and Applied Sciences, Buca 35160, Izmir, Turkey
[d]Izmir Katip Celebi University, Department of Materials Science and Engineering, Cigli 35620, Izmir, Turkey
[e]Hitit University, Department of Metallurgical and Materials Engineering, 19000 Çorum, Turkey
[f]Dokuz Eylul University, Department of Nanoscience and Nanoengineering, Buca 35160, Izmir, Turkey

Received 14 May 2013; received in revised form 8 July 2013; accepted 9 July 2013
Available online 18 July 2013

**Abstract**

Nanoporous titanium oxide ($TiO_2$) layers were fabricated on commercially pure titanium (Cp-Ti) substrates by the anodic oxidation method under a potentiostatic regime. Anodic oxidation was performed in an aqueous solution containing 1 wt% hydrofluoric acid at room temperature for 30 min. Subsequently one of the anodized samples was annealed at 480 °C for 2 h in air in order to obtain anatase transformation and increased crystallinity. The average pore diameter of both anodized and anodized+annealed samples were found to be nearly 52 nm and 66 nm, whilst the average inter-pore distances were approximately 65 nm and 76 nm, respectively. Characterization of nanoporous $TiO_2$ layers was carried out through X-ray diffractometer (XRD), scanning electron microscopy (SEM), atomic force microscopy (AFM) and UV visible spectroscopy. Effects of heat treatment on properties such as crystallinity, morphology and photocatalytic activity were investigated in details. Finally photocatalytic degradation ratios and changes in degradation kinetics under the presence of both anodized and anodized+annealed catalysts were calculated. Depending on the obtained results, the annealed film with anatase structure demonstrated highly efficient photacatalytic performance.


*Keywords:* Nanoporous titanium oxide; Anatase; Anodic oxidation; Photocatalytic activity; Methylene blue

## 1. Introduction

Titanium dioxide ($TiO_2$) has been widely investigated as a key material for photocatalytic, photovoltaic, bio-coating and photoelectrolytic applications due to its non-toxicity, chemical stability, low cost optical, electronic and physiochemical properties [1–5]. Since the discovery of photocatalytic water splitting on $TiO_2$ by Fujishima and Honda in 1972, the studies performed on $TiO_2$ as a photocatalyst for purification of groundwater and waste water have grown [6–11]. Nanostrucutured materials have attracted remarkable interest owing to their potential applications in micro-electronics, optical electronics and photocatalysis [12]. Many methods have been developed for the fabrication of $TiO_2$ nanotubes with larger surface areas, including anodic oxidation, template method, hydrothermal and soft chemical process [13–16]. Anodic oxidation is an effective method for producing $TiO_2$ nanotubes/nanopores with controllable pore sizes and morphologies because of low cost and simple fabrication [17].

It is well known that $TiO_2$ has three crystalline forms such as anatase, rutile and brookite. Among these three crystalline forms, anatase phase has been extensively used in photodegradation due to its high photoactivity [18–20]. Post-annealing is an important issue to transform the anodized $TiO_2$ nanotube

*Corresponding author at: Dokuz Eylul University, Department of Metallurgical and Materials Engineering, Buca 35160, Izmir, Turkey.
Tel.: +90 2323017476; fax: +90 2323017452.
*E-mail addresses:* m.erol@deu.edu.tr, tuncay.dikici@ikc.edu.tr (M. Erol).
*URL:* http://kisi.deu.edu.tr/m.erol/ (M. Erol).

0272-8842/$ - see front matter © 2013 Elsevier Ltd and Techna Group S.r.l. All rights reserved.
http://dx.doi.org/10.1016/j.ceramint.2013.07.046

arrayed films from amorphous in to crystalline structure [17]. In this study, we investigated the photocatalytic activity and the kinetics of amorphous and crystalline nanoporous $TiO_2$ films formed on pure titanium discs in hydrofluoric acid (HF) aqueous solution via constant voltage on degradation of methylene blue (MB).

## 2. Experimental details

Commercially pure titanium (Grade 2, Bagsan Co., Turkey) disc (diameter of 15 mm; thickness of 1 mm) was used as a substrate. All substrates were mechanically polished with 80-grit–2000-grit emery paper, and then washed with acetone, ethanol and distilled water in an ultrasonic cleaner. Prior to the experiments, acid activation was performed in a mixture of nitric acid ($HNO_3$) and hydrofluoric acid (HF) solutions for 10 s to remove the air-formed oxide layer.

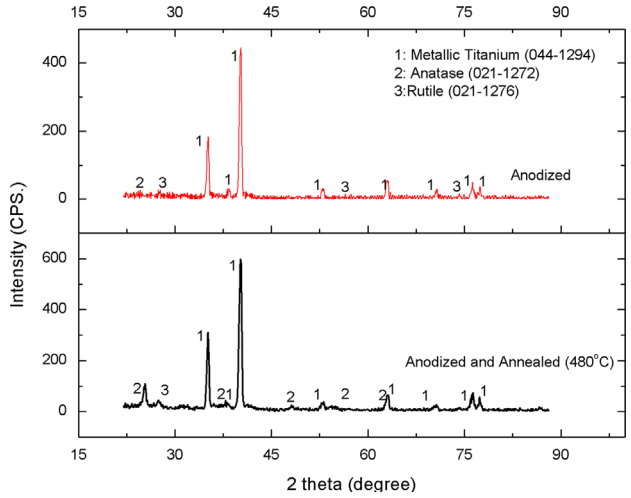


Fig. 1. XRD patterns of the anodized and anodized+annealed samples.

Anodization was performed in a two-electrode configuration under a constant 20 V anodic potential for 0.5 h at room temperature by a DC power supply (CRS Power, Turkey) and 1 (wt%) HF as an electrolyte. The distance between the anode and cathode was kept at about 40 mm. After the anodic oxidation, one of the anodized substrates was annealed at 480 °C for 2 h under air ambient to improve the crystallinity and anatase transformation.

X-ray diffraction (XRD, Rigaku D/MAX-2200/PC) patterns of the specimens were determined to identify phase structure by means of a diffractometer with a $CuK_\alpha$ irradiation. The surface morphology of the specimens was characterized by a scanning electron microscopy (SEM, JEOL 6060) and an atomic force microscopy (AFM, EasyScan2, Nanoscience) in contact mode.

Photocatalytic degradation experiments of the specimens were performed using a setup including aquous MB solutions for both catalysts and a UV light source (Osram, UltraVitalux E27, 300 W). In order to record catalyst-free degradation of MB under radiation an arbitration sample of the solution was also prepared. In this study, MB was supplied from Merck in the laboratory grade and used without further purification. 30 mL of MB solutions ($C_0 = 1.28 \times 10^{-5}$ mol/L) were poured into beakers and catalysts were placed across to the light source with a distance approximately 200 mm. As denoted in

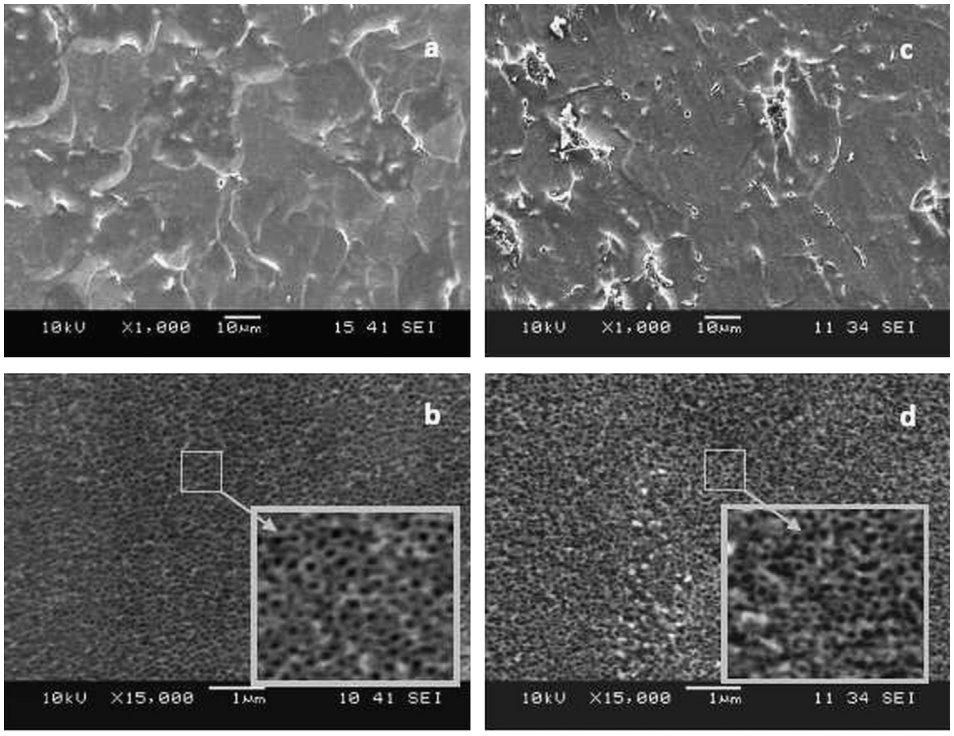


Fig. 2. SEM micrographs of the samples from (a) top view of anodized sample, (b) high-magnification top view of anodized sample, (c) the annealed sample at 480 °C after anodizing and (d) high-magnification top view of the annealed sample at 480 °C after anodizing.

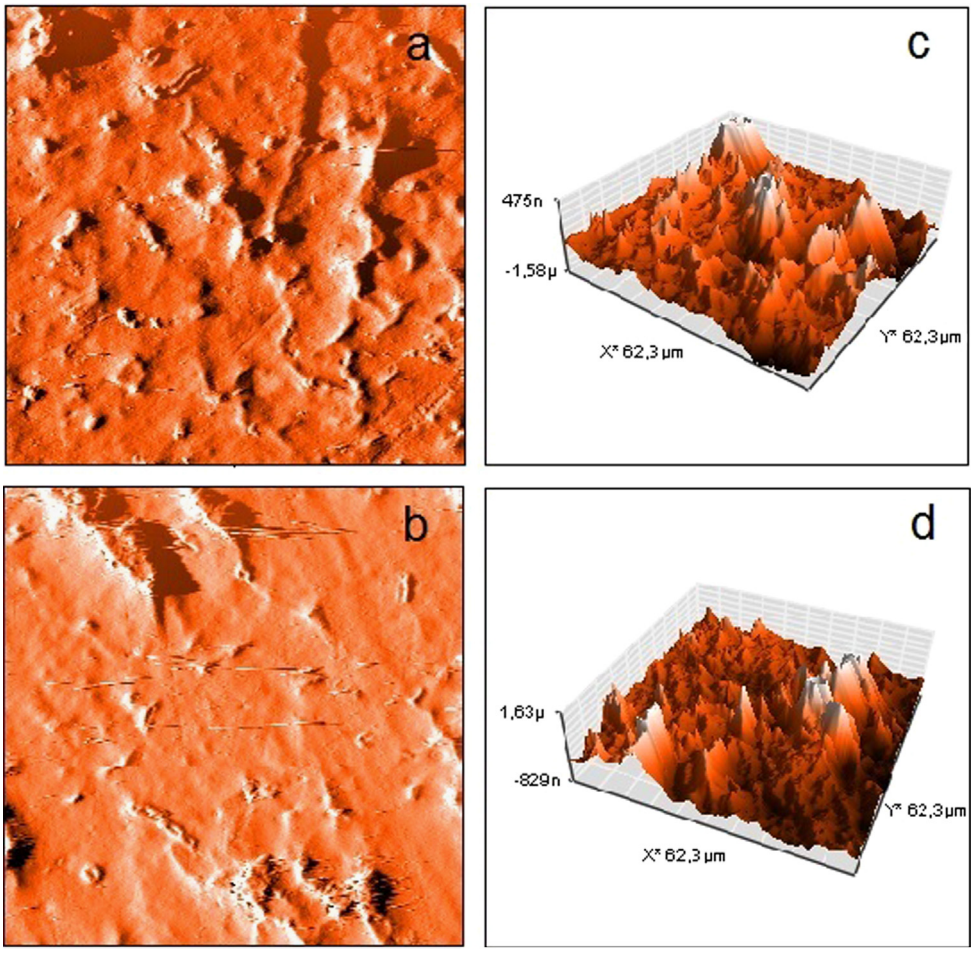


Fig. 3. AFM micrographs showing the topography of (a), (b) anodized samples (c) and (d) anodized+annealed samples.

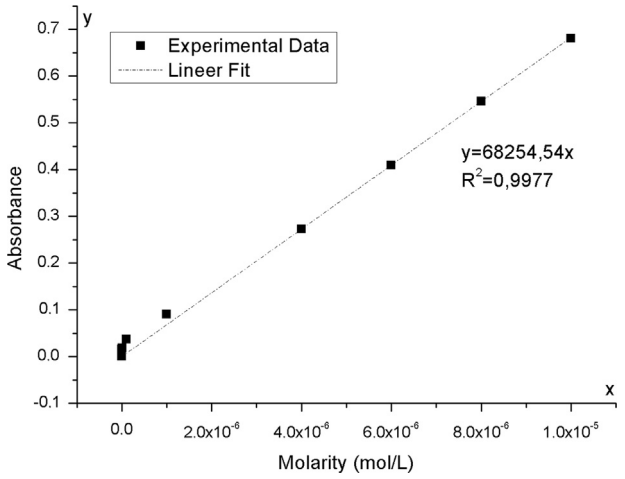


Fig. 4. Lambert–Beer correlation curve for MB solutions.

Lambert–Beer law; molarity of a solution is directly proportional to its absorbance [23]. In order to demonstrate the proportionality of the law with an experimental study, several MB solutions with molarities changing from $10^{-5}$ M to 0 M were prepared. The absorbance measurement of the solutions at 664 nm (which is maximum absorption wavelength of MB), were performed with a UV–visible spectrophotometer (V-530 JASCO UV/VIS). Subsequent to absorbance measurement, a calibration curve of MB solutions were plotted which shows the proportionality of measured absorbance values with known molarities.

Following the calibration process, to compare catalyst and post-treatment effect on photocatalytic efficiency three different samples were defined as SP0, SP1 and SP2 which are catalyst free, anodized and anodized+annealed samples, respectively. Time versus molarity values of all degraded photocatalytic

Table 1
Change in absorbance values and calculated molarities for different durations.

| Time (h) | *A*, Absorbance (664 nm) | | | *C*, Molarity (mol/L) | | |
|---|---|---|---|---|---|---|
| | (SP0) | (SP1) | (SP2) | (SP0) | (SP1) | (SP2) |
| **0** | 0.882 | 0.882 | 0.882 | $1.28 \times 10^{-5}$ | $1.28 \times 10^{-5}$ | $1.28 \times 10^{-5}$ |
| **5** | 0.633 | 0.482 | 0.281 | $9.27 \times 10^{-6}$ | $7.03 \times 10^{-6}$ | $4.10 \times 10^{-6}$ |
| **10** | 0.483 | 0.331 | 0.112 | $7.07 \times 10^{-6}$ | $4.83 \times 10^{-6}$ | $1.61 \times 10^{-6}$ |
| **15** | 0.343 | 0.207 | 0.031 | $5.02 \times 10^{-6}$ | $2.93 \times 10^{-6}$ | $4.39 \times 10^{-7}$ |
| **20** | 0.252 | 0.125 | 0.015 | $3.66 \times 10^{-6}$ | $1.83 \times 10^{-6}$ | $2.19 \times 10^{-7}$ |

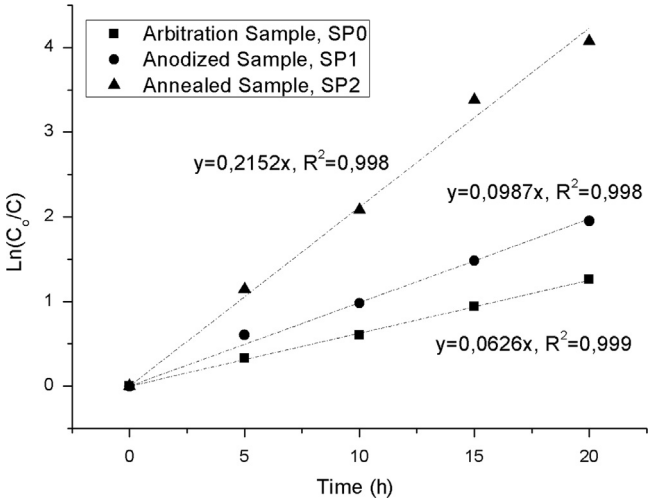


Fig. 5. Reaction kinetics′ comparision of the samples.

systems were recorded for different durations. Finally, photocatalytic degradation efficiencies and ratios were calculated using the absorbance—molarities calibration plot and chemical kinetic equations, respectively.

## 3. Results and discussion

It is well known that phase transformations and microstructure are of great influence on catalysts′ photocatalytic activity and photoelectrochemical properties as reported elsewhere [21]. Hence, XRD patterns of the specimens were revealed to show the effects of both anodizing and annealing on phase structure. According to patterns depicted in Fig. 1, it can be expressed that anodized sample was constructed from little amounts of anatase and rutile if compared to post annealed one. The peaks for metallic titanium substrates were also obtained in both patterns inasmuch as the thickness of the film is in nanoscale similar to Refs. [22,23].

Surface properties of a catalyst possess a key role on the performance because all the photocatalytical reactions ocurred on the surface [24], with this manner the obtained SEM and AFM microstructures were taken as follows. Fig. 2 shows the SEM micrographs of the samples with and without heat treatment after anodic oxidation treatment. Fig. 2a and c shows that the resulting films consist of self organized nanopores with an average diameter of ~60 nm and a wall thickness of ~70 nm. Fig. 3a–d shows two- and three-dimensional AFM images of anodized and anodized+annealed titanium samples. Both anodized and anodized+annealed samples have some craters distributed randomly. The regarding microstructures depict that there does not exist distinct changes in the microstructure by annealing process which supports effect of phase transformation as metioned elsewhere.

Generally photocatalytical performances of the catalyst were tested using artifactual dyes as impurities with the aim of waste water demonstration. By this way, MB was choosen as an artifactual dye in the present study. Prior to derivation of photocatalytic degradation efficiencies of the films on MB, As mentioned in the experimental study section, Lambert–Beer correlation curve showing linear relation between absorbance and concentration was plotted in Fig. 4. According to figure a linear function as $y=68254.54x$ was obtained with $R^2=0.9977$ where $x$, $y$, and $R$ denotes molarity absorbance and mean square errors, respectively. In order to determine photocatalytic degradation performances of UV irradiated SP0, SP1 and SP2 systems, 5 $mm^3$ of them were taken to measure maximum absorbance values at 664 nm for every 5 h after the starting time ($t_o$). Measured absorbance values were converted to concentration values for any UV irradiation durations by using this function. Changes in absorbance and calculated molarities of the mentioned systems for different durations are listed in Table 1. According to Table 1 it can be expressed that SP2 system with the smallest absorbance and the molarity at 20th hour, is the best catalyst if compared SP0 and SP1.

Rate of a photochemical reaction is a significant issue for any industrial design and photo-reactor based devices. Thus, kinetical behaviors of the samples are also calculated using basic kinetic equations according to the data listed in Table 1. The results depicted in Fig. 5 indicate that the kinetics of photocatalytic reaction fit the Langmiur–Hinshelwood kinetics model. Therefore, the absorption of MB on nanotube array surface is the controlling step in the whole degradation process [25]. Three different functions were obtained where $x$ and $y$ denotes time and $\mathrm{Ln}(C_0/C)$ respectively. According to the linear fitting processes, the rate constants were calculated as 0.2152, 0.0987 and 0.0626 for SP0, SP1 and SP2, respectively. Photocatalytic degradation efficiencies of the samples were also calculated using equation; $100-((100C-C_0)/C)$ where $C_0$ and $C$ are the initial and concerning molarities of duration respectively. Calculated efficiency changes versus time for the samples are also represented in Fig. 6. As mentioned beforehand, the SP2 sample with more anatase content was found to be more effective than that with the SP1. This effectiveness can be seen in both Figs. 5 and 6. Finally it can be inferred that phase structure is more effective than the morphology depending on the obtained results.

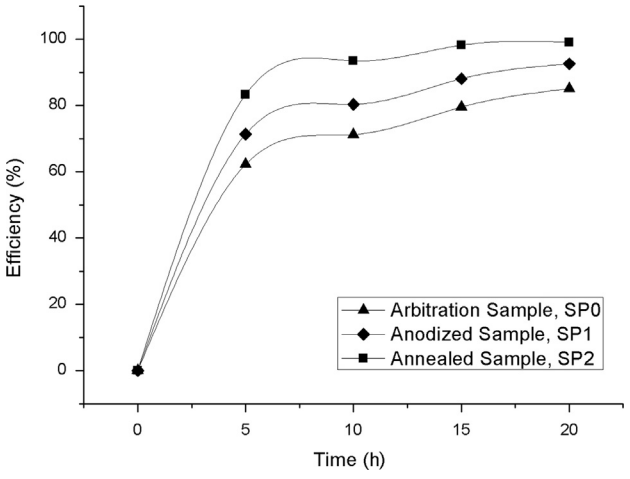


Fig. 6. Photocatalytic degradation efficiencies of the samples.

## 4. Conclusions

To sum up, the films with nanoporous structured $TiO_2$ were successfully produced on the Ti substrates by the anodic oxidation method. The anodic oxidation was carried out in the electrolyte containing HF at 20 V for 30 min. After the anodization process, the nanopores have amorphous oxide structure, but they were transformed into anatase by annealing in air at 480 °C for 2 h. In the scope of the obtained results, the annealed samples which consisted of crystalline anatase have been reported as the most efficient for MB degradation. In addition to the structural results it can be inferred for the microstructure that, $TiO_2$ nanoporous array which is the nature of anodization—is not destroyed with the heat treatment. The nanopore arrayed (with increased catalyst surface in contact with degraded solution) $TiO_2$ films can be inferred as good candidates′ for photocatalytic degradation of the hazardous organic impurities in waste water. Beside experimental results, in the manner of the processing technology, anodization of titanium can be an innovative approach for the bulk production and commercialization of photocatalytic reactors or systems.

## Acknowlegement

The authors are indebted to State Planning Foundation (DPT) and Dokuz Eylul University for financial and infra-structural support for establishment of Dokuz Eylul University, Center for Production and Applications of Electronic Materials (EMUM) where this research was carried out.

## References

[1] A. Fujishima, T.N. Rao, D.A. Tryk, Titanium dioxide photocatalysis, Journal of Photochemistry and Photobiology C 1 (2000) 1–21.
[2] R. Asahi, Y. Taga, W. Mannstadt, A.J. Freeman, Electronic and optical properties of anatase $TiO_2$, Physical Review B 61 (2000) 7459–7465.
[3] M. Adachi, Y. Murata, I. Okada, S. Yoshikawa, Formation of titania nanotubes and applications for dye-sensitized solar cells, Journal of the Electrochemical Society 150 (2003) 488–493.
[4] S.H. Oh, R.R. Finones, C. Daraio, L.H. Chen, S. Jin, Growth of nano-scale hydroxyapatite using chemically treated titanium oxide nanotubes, Biomaterials 26 (2005) 4938–4943.
[5] A. Fujishima, K. Honda, Electrochemical photolysis of water at a semiconductor electrode, Nature 238 (1972) 37–38.
[6] Y.H. Hsien, C.F. Chang, Y.H. Chen, S. Cheng, Photodegradation of aromatic pollutants in water over $TiO_2$ supported on molecular sieves, Applied Catalysis B-Environmental 31 (2001) 241–249.
[7] M. Kositzi, I. Poulios, S. Malato, J. Caceres, A. Campos, Solar photocatalytic treatment of synthetic municipal wastewater, Water Research 38 (2004) 1147–1154.
[8] O. Prieto, J. Fermoso, Y. Nuěez, J.L. Del Valle, R. Irusta, Decolouration of textile dyes in wastewaters by photocatalysis with $TiO_2$, Solar Energy 79 (2005) 376–383.
[9] A.L. Linsebigler, G. Lu, J.T. Yates, Photocatalysis on $TiO_2$ surfaces: principles, mechanisms, and selected results, Chemical Reviews 95 (1995) 735–758.
[10] K. Kabra, R. Chaudhary, R.L. Sawhney, Treatment of hazardous organic and inorganic compounds through aqueous-phase photocatalysis: a review, Industrial and Engineering Chemistry Research 43 (2004) 7683–7696.
[11] X.J. Li, J.W. Cubbage, W.S. Jenks, Photocatalytic degradation of 4-chlorophenol. 2. The 4-chlorocatechol pathway, Journal of Organic Chemistry 64 (1999) 8525–8536.
[12] S.J. Tans, A.R.M. Verschueren, C. Dekker, Room-temperature transistor based on a single carbon nanotube, Nature 393 (1998) 49–52.
[13] Q. Cai, L. Yang, Y. Yu, Investigations on the self-organized growth of $TiO_2$ nanotube arrays by anodic oxidization, Thin Solid Films 515 (2006) 1802–1806.
[14] J. Qiu, Z. Jin, Z. Liu, X. Liu, G. Liu, W. Wu, X. Zhang, X. Gao, Fabrication of $TiO_2$ nanotube film by well-aligned ZnO nanorod array film and sol-gel process, Thin Solid Films 515 (2007) 2897–2902.
[15] H. Zhang, G.R. Li, L.P. An, T.Y. Yan, X.P. Gao, H.Y. Zhu, Ferromagnetism of co-doped $TiO_2$(B) nanotubes, Journal of Physical Chemistry C 111 (2007) 6143–6148.
[16] M. Wei, H. Zhou, Y. Konishi, M. Ichihara, H. Sugiha, H. Arakawa, Synthesis of tubular titanate via a self-assembly and self-removal process, Inorganic Chemistry 45 (2006) 5684–5690.
[17] D. Gong, C.A. Grimes, O.K. Varghese, W. Hu, R.S. Singh, Z. Chen E.C. Dickey, Titanium oxide nanotube arrays prepared by anodic oxidation, Journal of Materials Research 16 (2001) 3331–3334.
[18] L.M. Shen, N.Z. Bao, Y.N. Zheng, A. Gupta, T.C. An, K. Yanagisawa, Journal of Physical Chemistry C 112 (2008) 8809.
[19] H.W. Kim, H.S. Kim, H.G. Na, J.C. Yang, D.Y. Kim, Growth, structural, raman, and photoluminescence properties of rutile $TiO_2$ nanowires synthesized by the simple thermal treatment, Journal of *A*lloys and Compounds 504 (2010) 217–223.
[20] A. Fahmi, C. Minot, B. Silvi, M. Causa, Theoretical analysis of the structures of titanium dioxide crystals, Physical Review B 47 (1993) 11717–11724.
[21] H. Kyung-Jun, L. Jae-Wook, S. Wang-Geun, J.H. Dong, L. Se-Il, Y. Seung-Joon, Adsorption and photocatalysis of nanocrystalline $TiO_2$ particles prepared by sol–gel method for methylene blue degradation, Advanced Powder Technology 23 (2012) 414–418.
[22] Y. Jiaguo, W. Bo, Effect of calcination temperature on morphology and photoelectrochemical properties of anodized titanium dioxide nanotube arrays, Applied Catalysis B: Environmental 94 (2010) 295–302.
[23] O. Kinji, A. Teruo, T. Teruki, High-performance photocatalyst prepared from metallic titanium, Welding International 23 (2009) 323–327.
[24] M. Erol, O. Sancakoglu, M. Yurddaskal, S. Yildirim, E. Çelik, A comparison on physical, structural, and photocatalytical properties of $TiO_2$ nanopowders produced using sol-gel and flame spray pyrolysis, International Journal of Applied Ceramic Technology, http://dx.doi.org/10.1111/ijac.121/ijac.12018, in press.
[25] S. Jianhui, W. Xiaolei, S. Jingyu., S. Ruixia, S. Shengpeng, Q. Liping, Photocatalytic degradation and kinetics of orange G using nano-sized Sn (IV)/$TiO_2$/AC photocatalyst, Journal of Molecular Catalysis A: Chemical 260 (2006) 241–246.